TAO, Vol.4, No.4, 367-380, December 1993

Downhole Instrument Orientations and Near Surface Q Analysis From the SMART2 Array Data

HAN-YIH PENG[1] and KUO-LIANG WEN[2]

(Manuscript received 22 August 1993, in final form 20 December 1993)

ABSTRACT

Installation of the SMART2 downhole array in Da-Han Industrial School was completed in May 1992. This array contains one free surface station and three downhole accelerometers down to 200 m depth. Thirteen events recorded by this downhole array are used to study the orientations of the downhole instruments by cross-correlation method. The results show the longitudinal direction of the instruments at 50 m, 100 m, and 200 m depths of downhole accelerometers are N3°E, N91°E, and N75°E, respectively. The near surface Q value is calculated by using the records of three events. The result of $Q(f)=9.55f^{1.06}$ was obtained from the smoothed power spectrum ratios. The surface ground motions of two events are simulated from the observed downhole records and Q value we obtained by using the Haskell method. The results confirm the downhole instrument orientations and near surface Q value that we derived in this study.

1. INTRODUCTION

There are several studies about finding Q value near the surface in California by comparing the downhole ground motion with the surface ground motion, including Hauksson *et al.* (1987) (Q_b=25 average between 1500 m and 420 m depth), Malin *et al.* (1988) (Q_b=9 between 0 and 500 m depth), Seale and Archuleta (1989) (Q_b=10 between 0 and 166 m depth), Gibbs and Roth (1989) (Q=4 between 57 and 102 m depth), Fletcher *et al.* (1990) (Q_b=8 at one and 11 at the others in the upper 50 m) and Archuleta *et al.* (1992) (Q=12 in the upper 200 m), they all found very low Q values near the surface. Recently, Wang (1993) reviewed Q values in Taiwan and pointed out that the Q values of the sediments can be made for further studies. Chang and Yeh (1983) using strong motion data found $Q(f)=98f^{1.0}$ in the upper 11 km and $Q(f)=225f^{1.1}$ in the upper 80 km for northeast Taiwan. The only study of the near surface Q in Taiwan was done by using the SMART1 array data

[1] Institute of Geophysics, National Central University, Chung-Li, Taiwan, R.O.C.

[2] Institute of Earth Sciences, Academia Sinica, P.O. Box 1-55, Nankang, Taipei, Taiwan, R.O.C.

in the Lotung area (Shieh, 1992). The SMART2 array (Chiu and Yeh, 1991) is located in the Hualien area. Three downhole accelerometers are installed in the Da-Han Industrial School at depths of 50 m, 100 m, and 200 m. This downhole array gives us an opportunity to study the near surface Q value in the Hualien area. The orientations of the downhole instruments are not measured since the installation. Before doing the Q value study, we must solve the problem of the downhole instrument orientations. Several methods had been used to check the downhole instrument orientation, for example, polarization method (Vidale, 1986) and cross-correlation method (Yamazaki *et al.*, 1992). In this study, we used the cross-correlation method to estimate the instrument orientations of the downhole array. To check the estimated value of instrument orientation and Q value, we used the Haskell method to simulate surface ground motion by using the downhole record as input motion. From the similarity between the synthesized results and the observed records, we can show the exactness of the instrument orientations and near surface Q value we obtained.

2. DOWNHOLE ARRAY AND DATA

The SMART2 downhole array is located in the Da-Han Industrial School in the Hualien area. This array consists of one free surface and 3 downhole accelerometers whose depths are 50 m, 100 m, and 200 m. The four FBA sensors are connected to two 6-channel SSR-1 digital recorders. Each recorder has 16 bits resolution and the sampling rate is 200 points/sec. An Omega clock timing system provides one ms accuracy and continuously synchronizes the clock to standard time.

The SMART2 downhole array began operating on May 6, 1992. From this date through Sep. 1, 1992, thirteen earthquakes were recorded by this downhole array (Table 1). These events are used to calculate the instrument orientations of the downhole array. Figure 1 shows the location of the downhole array and epicenters. Most of the records are too weak to do the near surface Q and simulation study, but five of them were strong enough for our study. In these five events, the M_L are larger than 4.5 and the peak ground accelerations of their EW and NS components are larger than 5.0 gals for the station at depths of 200 m. On the basis of the in situ soil boring and downhole velocity logging (Chung-Chi Technical Consultant Co. 1991), the average shear wave velocity profiles as well as the geological columnar sections are shown in Figure 2. The geological profile includes four layers. The first consists of brown medium-coarse sand with small gravel, the second is gravel and gray mud with some medium-coarse sand, the third is sand with thin clay and small gravel, and the fourth layer includes rock, pebble gravel and medium-coarse sand.

3. DOWNHOLE INSTRUMENT ORIENTATIONS

The problem of downhole instrument orientation is solved by using the maximum cross-correlation method. This is a four-dimensional problem, include three components and time lag, as Yamazaki *et al.* (1992) has shown. For SMART2 downhole array, time lag was obtained by in situ velocity logging and the orientation error is very small in vertical direction based on the in situ geotechnical survey (Chung-Chi Technical Consultant Co., 1991). So, in this study the problem can be simplified to a two dimensional problem that only needs analysis of the records of two horizontal components. The earthquake ground motion at a point is represented by a vector $z(t)=[z_1(t),z_2(t)]$. $z_1(t)$ and $z_2(t)$ indicating the ground motion

Table 1. Event parameters recorded by the SMART2 downhole array.

EVENT NO.	ORIGIN TIME (UT)	EPICENTER	DEPTH (km)	M_L	PGA*(gal)			NOTE
					V	T	L	
1	1992 05 21 05:04:35.25	121-32.69E 23-43.92N	16.7	4.5	1.17	3.31	1.93	O.
2	1992 05 31 13:16:48.86	121-23.08E 23-52.29N	12.6	4.5	1.88	2.72	2.04	O.
3	1992 06 01 04:50:14.98	121-32.32E 23-49.68N	4.6	4.3	1.55	2.97	3.09	O.
4	1992 06 08 04:58:07.20	121-38.14E 23-58.44N	23.1	4.0	3.55	4.50	6.04	O.
5	1992 06 25 18:29:11.12	121-37.92E 24-01.16N	22.7	4.8	20.21	27.77	28.63	O. S.
6	1992 06 25 19:37:41.95	121-31.18E 24-05.24N	13.4	3.8	3.63	6.63	7.75	O.
7	1992 06 30 13:07:41.15	121-46.13E 24-08.41N	28.6	4.8	2.49	3.81	5.24	O.
8	1992 07 07 00:45:33.30	121-53.16E 24-22.52N	57.8	4.9	1.58	2.41	2.96	O.
9	1992 07 23 21:03:35.07	121-24.08E 23-57.74N	12.8	4.8	1.51	2.85	2.40	O.
10	1992 07 24 05:26:55.86	121-49.96E 24-03.21N	30.0	5.1	4.12	6.55	5.35	O. Q.
11	1992 08 08 19:37:52.39	121-37.51E 23-56.07N	11.7	4.6	6.00	11.27	8.95	O. Q.
12	1992 08 14 17:26:25.11	121-33.13E 24-06.38N	15.7	4.8	18.97	30.77	48.78	O. Q.
13	1992 09 01 16:41:15.21	121-46.40E 23-42.70N	51.4	5.2	7.64	22.13	23.71	O. S.

O. : Orientation calculation.
Q. : Q value analysis.
S. : Simulation study.
* : PGA recorded at the depths of 200 meters.

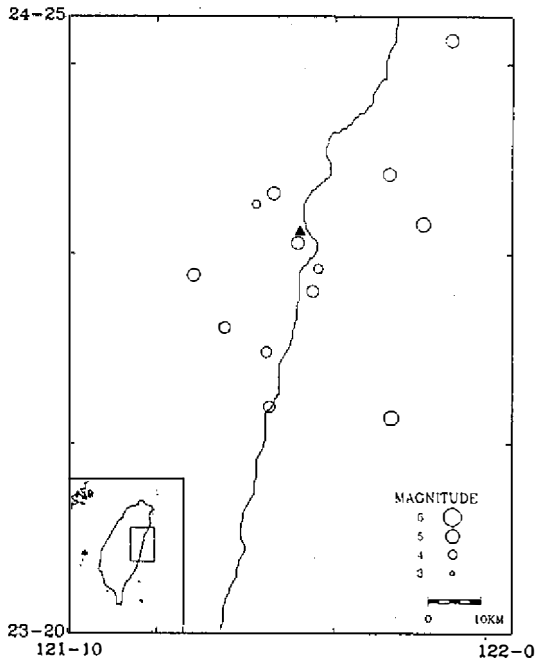

Fig. 1. Location of the SMART2 downhole array and epicenters.

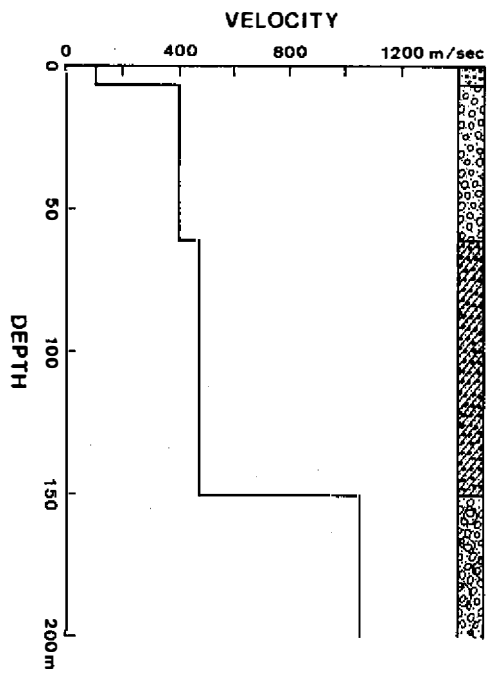

Fig. 2. Shear wave velocity profile and geological columnar section.

at the preassigned directions, i.e. north-south (NS) and east-west (EW). Suppose the ground motion y(t)=[y_1(t),y_2(t)] recorded by an instrument which has an angle α different from the preassigned direction. Than z(t) can be estimated from the observed y(t) by the product of the transform matrix

$$z(t) = T(\alpha)y(t), \tag{1}$$

the corresponding two-dimensional coordinate transform matrix can be obtained as

$$T(\alpha) = \begin{bmatrix} cos\alpha & sin\alpha \\ -sin\alpha & cos\alpha \end{bmatrix}, \tag{2}$$

where α is the angle waited to be solved.

If we want to decide the angle α, a reference station with known instrument orientation is necessary. For the next calculation, we consider a ground motion at the reference point x(t)=[x_1(t),x_2(t)]. If the reference point and the checking point are not far apart, within a few hundred meters, the existence of coherently propagating waves between the points can be assumed. The orientation difference angle α between reference station (x) and checking point (y) can be estimated by the maximum cross-correlation coefficient between x(t) and z(t) in the time domain. Since there only two horizontal components in these vectors are used, a sum of two cross-covariance function is considered

$$s(\alpha,\tau) = \sum_{i=1}^{2} R_{x_i z_i}(\tau) = \sum_{i=1}^{2} E[(x_i(t) - \bar{x}_i)(z_i(t+\tau) - \bar{z}_i)], \tag{3}$$

where E[.] means the ensemble average and τ is the time lag between x(t) and z(t). Substituting equation (1) into equation (3) results in

$$s(\alpha,\tau) = \sum_{i=1}^{2}\sum_{j=1}^{2} t_{ij} R_{x_i y_j}(\tau), \tag{4}$$

where t_{ij} is the element of the transformation matrix T in equation (1) and $R_{x_i y_j}(\tau)$ is defined as

$$R_{x_i y_j}(\tau) = E[(x_i(t) - \bar{x}_i)(y_j(t+\tau) - \bar{y}_j)]. \tag{5}$$

In evaluating equations (4) and (5) for the sample processes of x(t) and y(t), the temporal average is used instead of the ensemble average for convenience. Then equation (5) is replaced by

$$R_{x_i y_j}(\tau) = \frac{1}{n}\sum_{k=1}^{n} x_i(t_k)y_j(t_k+\tau) - \bar{x}_i\bar{y}_j, \tag{6}$$

and

$$\bar{x}_i = \frac{1}{n}\sum_{k=1}^{n} x_i(t_k); \bar{y}_j = \frac{1}{n}\sum_{k=1}^{n} y_j(t_k+\tau), \tag{7}$$

where n is the number of discretized steps.

At the Da-Han downhole array, the orientation of the surface instrument is known and can be used as the reference point. The time leg τ is obtained by in situ downhole velocity logging. The direction of the downhole instruments can be estimated by finding the maximum cross-correlation coefficient between the records of the reference point and downhole instruments with the time leg τ. The downhole records were rotated counterclockwise from 0° to 180° and 0° to -180° with 1° interval, and calculated the cross-correlation coefficient with surface record at each angle. The results are shown in Figure 3. The average results from all events show that the longitudinal directions of the downhole instruments at depths of 50 m , 100 m, and 200 m are N3°±7°E, N91°±10°E, and N75°±10°E, respectively .

Figure 4 shows an example of the velocity waveform. Two horizontal components of the downhole records are rotated to NS and EW directions, respectively, based on the angle we obtained. From this figure we can see that the waveforms are very consistent between surface and downhole station except peak values are a little different. This can show the accuracy of the angles we obtained.

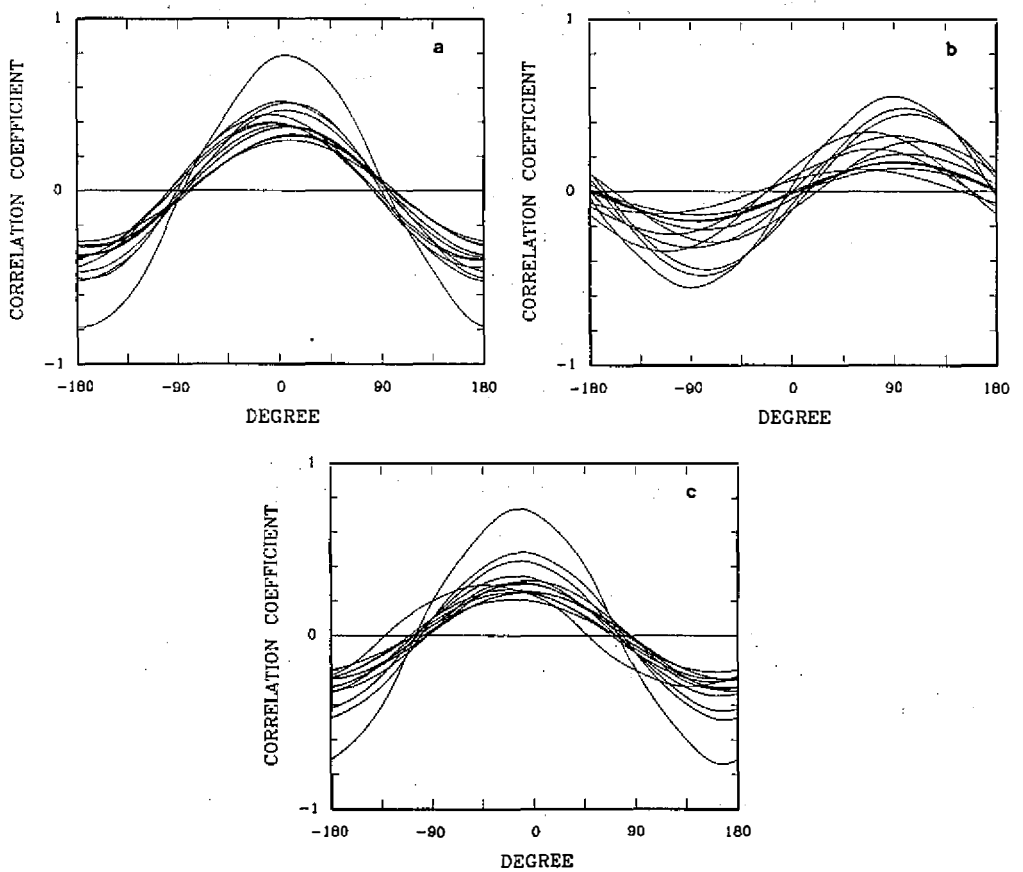

Fig. 3. Cross-correlation coefficient at different angles for the records of the station pairs between (a) surface and 50 m, (b) surface and 100 m, and (c) 100 m and 200 m depths.

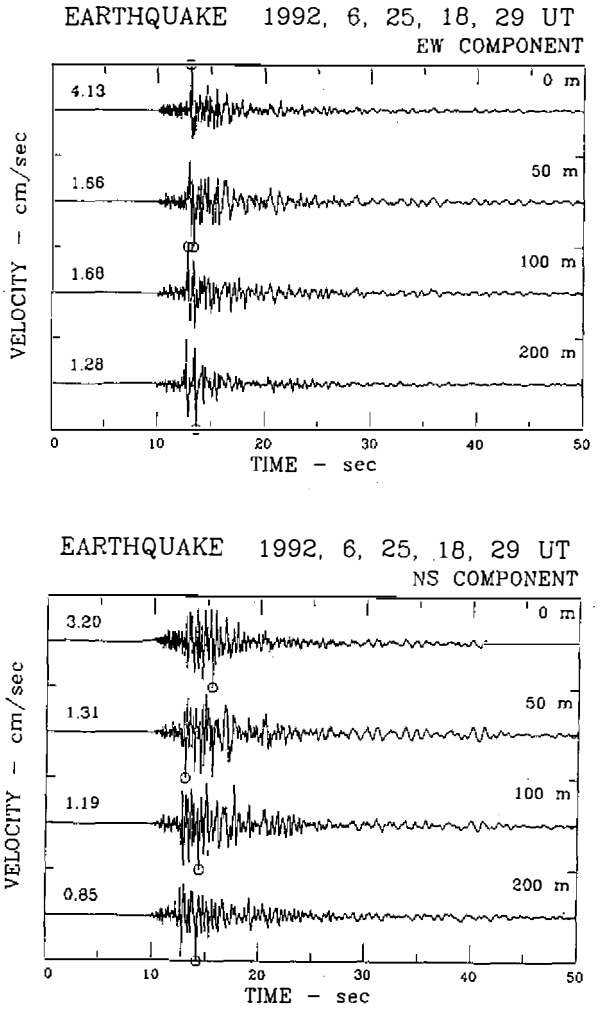

Fig. 4. **Examples of the velocity waveforms of event 5 after the orientation angle correction.**

4. Q VALUE

Frequency dependent Q was found by Aki and Chouet (1975) from studying the coda wave of earthquake in California and Japan. A relationship that Q grows with frequency proportionally as f^n was suggested by many authors (e.g., Der and McElfresh, 1977; Tsujiura, 1978; Rautian and Khalturin, 1978; Aki, 1980; Console and Rovelli, 1981; and Rodriguez *et al.*, 1983). For studying the Q value, we calculate the power spectra of the recorded accelerograms and take a smoothing procedure. A power spectrum is estimated by

$$|A(\omega)|^2 = A(\omega)A^*(\omega), \tag{8}$$

where $A^*(\omega)$ is the complex conjugate of $A(\omega)$, and $A(\omega)$ is the Fourier spectrum of the acceleration time history a(t). In this study, we use the time domain moving window method to smooth the power spectrum. The degree of smoothing depends on the window length. A shorter window length will result in a smoother spectrum (Bath, 1979). The window we use is cosine window, shown as in Figure 5, and the form is :

$$w(t) = 0.5(1 - cos(2\pi(t - t_1)/t_w)) \qquad t_1 \leq t < t_2, \tag{9}$$

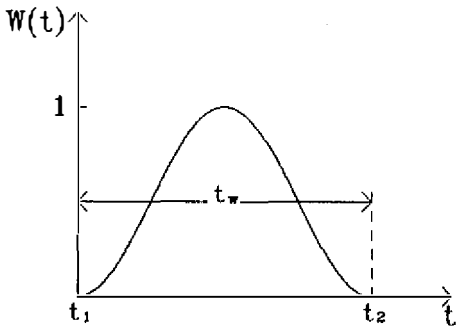

Fig. 5. Cosine window used in this study.

where t_1 and t_2 are low and high roll-off time, the window length t_w equal to (t_2-t_1) and the window shift length t_s is given as $t_w/2$. In this study, the Q value is defined as Q_s, so we rotated the horizontal components into tangential and radial components with the angle obtained by previous section. The power spectrum of a seismic wave, generated from seismic source, propagated through a dispersive medium and received by j-th station with epicentral distance R_j can be represented as (Aki and Chouet, 1975; Console and Rovelli, 1981)

$$S_j(f, R_j) = O(f)F(R_j)exp[-2\pi f R_j/(vQ(f))], \tag{10}$$

where O(f) is the source spectrum, F(R_j) represents the geometric spreading function, v is the group velocity of the wave in medium, and Q(f) stands for quality factor of the path. Considering the Q between two stations (in this study it is from 200 m depth to ground surface), the power spectrum ratio can be represented as:

$$\frac{S_1(f, R_1)}{S_2(f, R_2)} = \frac{F(R_1)}{F(R_2)} exp[-2\pi f \Delta R/(vQ(f))], \tag{11}$$

where subscripts 1 and 2 stand for surface and 200 m deep stations, respectively, Δ R=R_1-R_2. The 200 m distance compared to hypocentral distance is very small, so F(R_1)/F(R_2) can be assumed equal to 1 and $\Delta R/v$ equals the known time leg τ. Then the spectrum ratio can be represented as:

$$\frac{S_1(f)}{S_2(f)} = exp[-2\pi f \tau/Q(f)], \tag{12}$$

the Q(f) is replaced by

$$Q(f) = \frac{-2\pi f\tau}{ln(S_1(f)/S_2(f))}, \tag{13}$$

and the Q(f) can be represented as

$$Q(f) = a \cdot f^b, \tag{14}$$

where a and b are constants.

Before calculating the value of $S_1(f)/S_2(f)$ for obtaining the Q(f), we must consider the effects of amplification in the ground motions. Amplification due to the impedance contrast between two materials is a result of the conservation of energy (Carter *et al.*, 1984). Assuming complete transmission, the amplification factor for a plane wave traveling from medium 1 into medium 2 is

$$A = \sqrt{\frac{\rho_1 v_2}{\rho_2 v_2}} \tag{15}$$

where v and ρ are velocity and density respectively.

Using the velocities and densities obtained from in situ geotechnical survey (Chung-Chi Technical Consultant Co., 1991), the amplification factor between 200 m and ground surface layer can be calculated and was equal to 3. The free surface record was corrected by this amplification factor and free surface effect. The corrected record and the record at 200 m depth were used to calculate the near surface Q value. Figure 6 depicts the Q(f) values by different smoothing window length. From this figure, we can see that a shorter window length results in more convergence Q value at the higher frequency part. The Q values oscillated from 7 Hz to 40 Hz at the window length of 1 second (Figure 6a), and the oscillations decreased as the window length became shorter. More consistent results were obtained in the low frequency part for different window lengths. Through several tests, we selected 0.05 second time window for smoothing, and the least-square fit also shown in Figure 6d, and the result is $Q(f)=9.55f^{1.06}$. From Figure 6d we can see that the results of Q_o from event 10, 12, and 11 have become smaller. The magnitude of events 10, 12, and 11 are 5.1, 4.8, and 4.6, and the hypocentral depths are 30.0, 15.7, and 11.7 km, respectively. Theoretically, the spectral ratio can delete the source effect, but it may not remove it completely. This effect can include the standard deviation. If we use more events, it may show in the same error band. Comparing the hypocentral depths of these three events, we can see that the deeper event (event 10) has larger Q_o value. One possible reason is that the seismic wave from a deeper event will incident more vertically than that from a shallow event. So, the attenuation effect for the vertical incident wave will be smaller. This means that the Q_o value will be larger. Since this study has only three events, it does not prove this result. If we have more events we can do deeper discussion of this problem.

5. SIMULATION OF SURFACE GROUND MOTION

The exactness of the results of the downhole instrument orientations and the near surface Q(f) can be checked by using the downhole records as input motion to synthesize the surface ground motion through the Haskell method. On the basis of the directions we got,

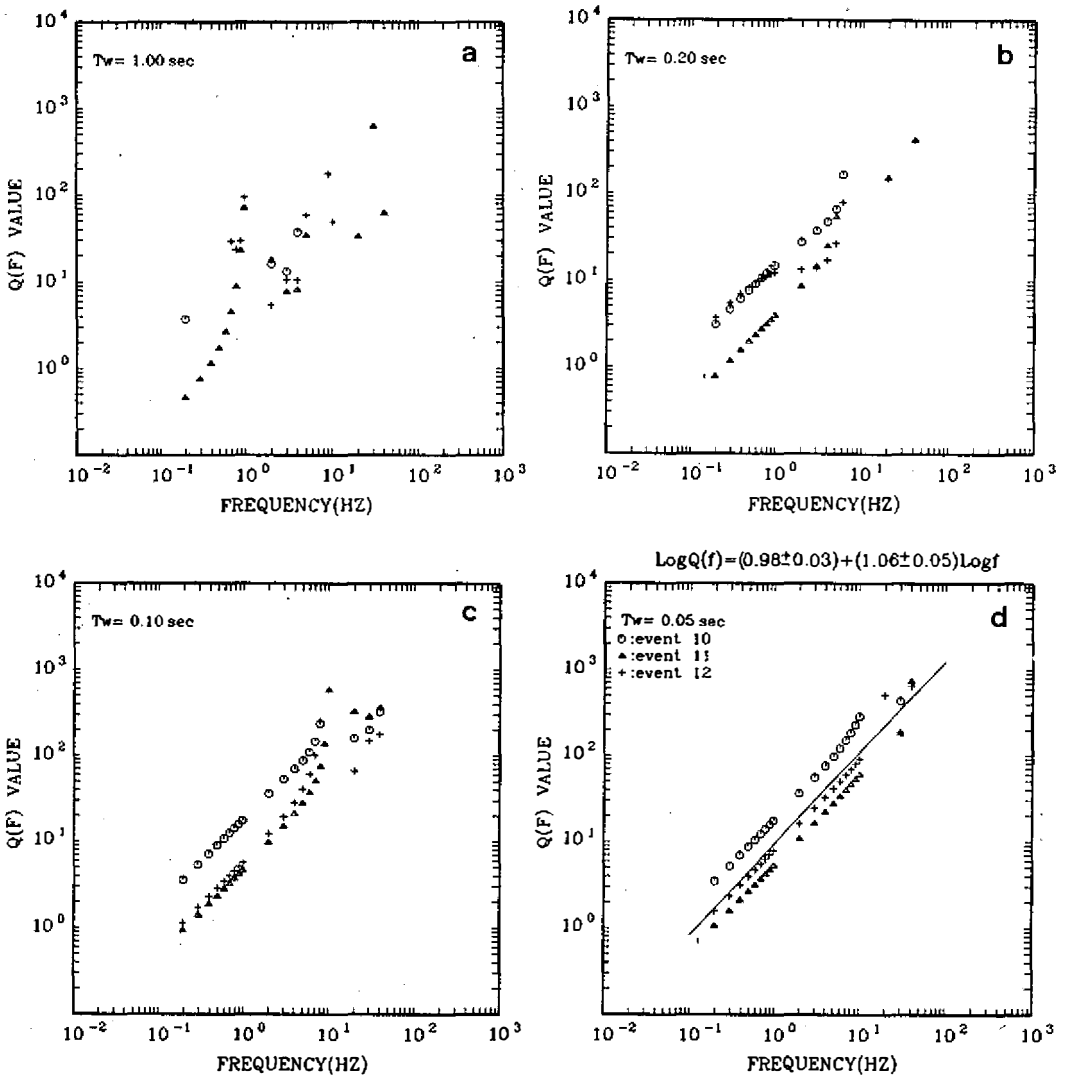

Fig. 6. Q Values calculated by using different smoothing window length. (a) 1.0 sec, (b) 0.2 sec, (c) 0.1 sec, and (d) 0.05 sec time window length.

the horizontal component records of events 5 and 13 are rotated into tangential and radial components. Then a bandpass filter from 0.2 Hz to 15 Hz is used to filter the records. Figures 7 and 8 show the results of the actual records compared with the synthetic seismogram (velocity time history) for events 5 and 13, respectively. Dash lines in each figure show the observation record at the ground surface is the same as the top trace in each figure. Comparing the synthetic and observed seismograms, we can see that the results by using the record at 50 m depths as input motion are better than those using deeper records. The simulation results for event 13 are better than those for event 5; that is because event 5 has more high frequency signals and not considers the free surface reflection wave as shown

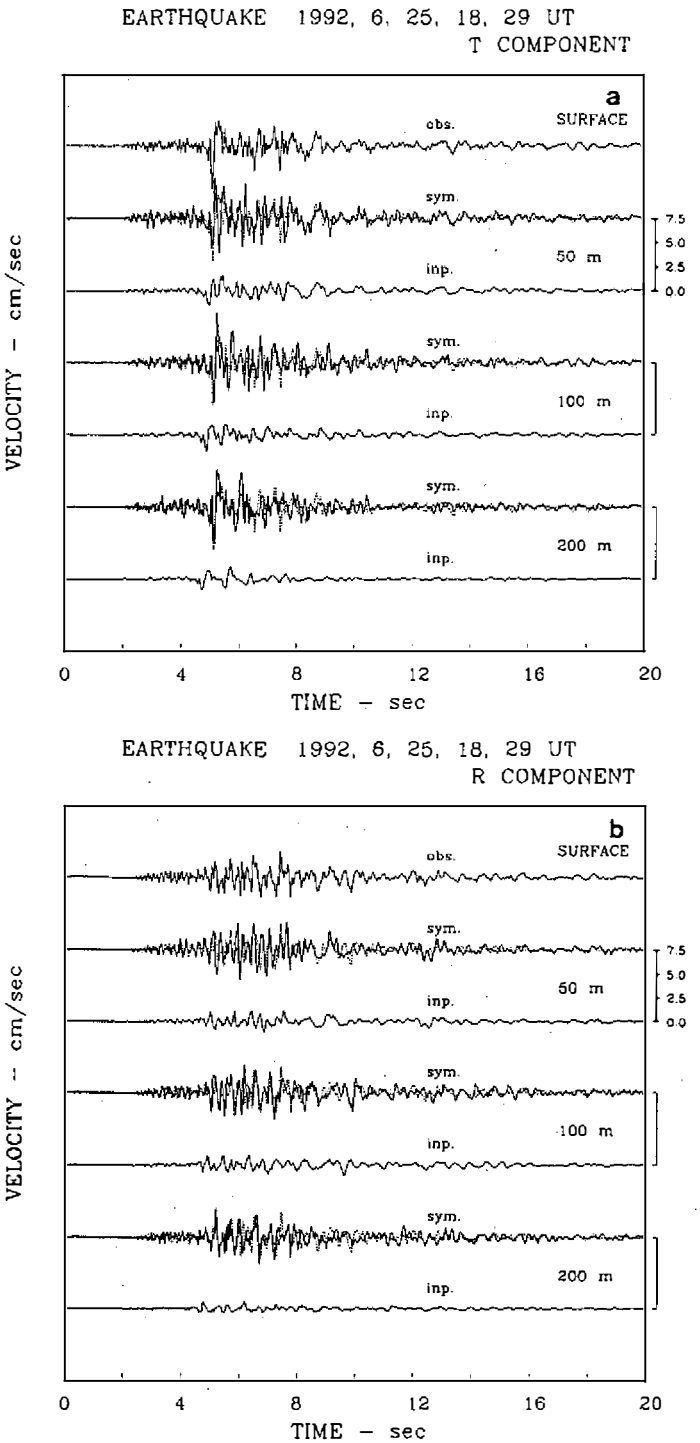

Fig. 7. Synthetic seismogram of (a) tangential and (b) radial components for event 5.

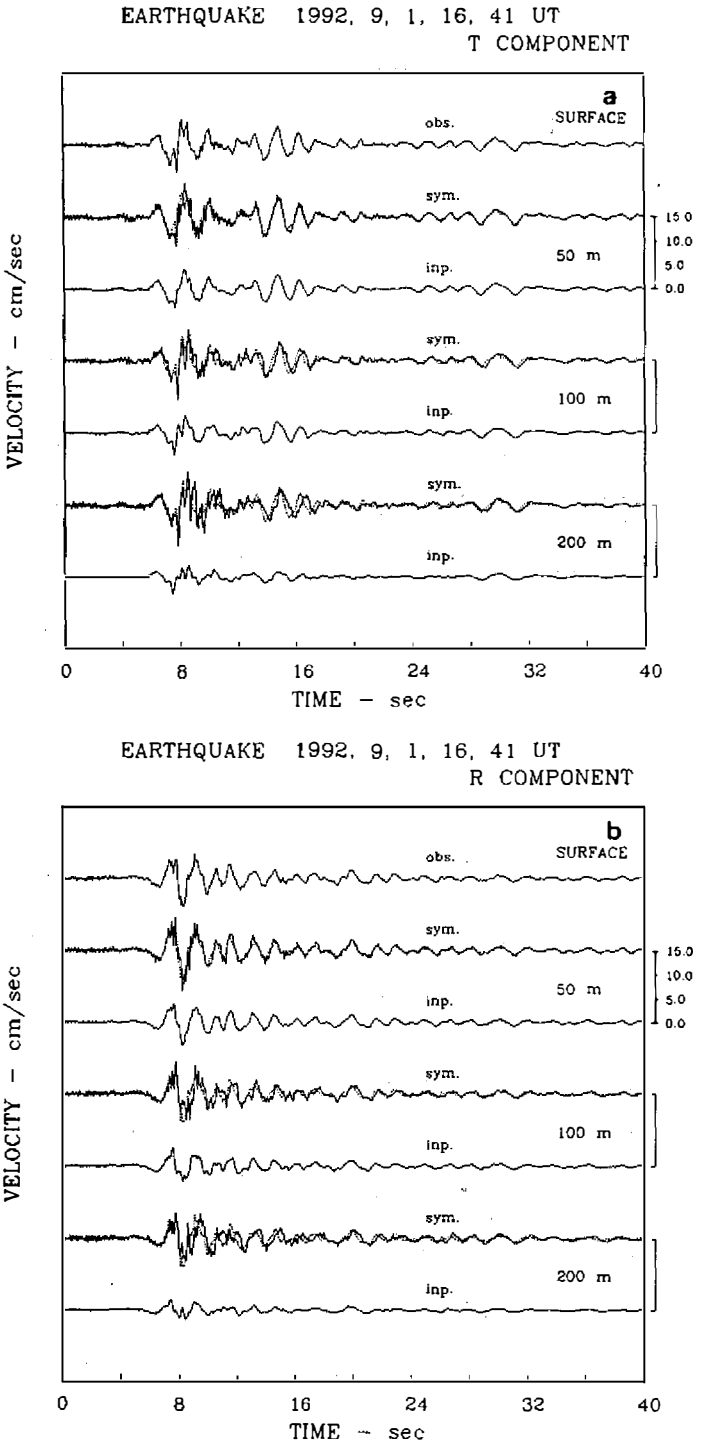

Fig. 8. Synthetic seismogram of (a) tangential and (b) radial components for event 13.

clearly in the records of event 5 (Figure 7). From Figure 8 we can see that although the later phase has a little shift, the amplitude still has very good fit. These simulation results show that the downhole instrument orientations and the frequency dependent Q obtained in this study are suitable for use.

6. CONCLUSION AND DISCUSSIONS

Since the installation of the SMART2 downhole array in Dan-Han Industrial School in the Hualien area, we have no idea about the downhole instrument orientations. In this study, we use the earthquake records to solve this problem and calculate the Q value through the spectral ratio method.

On the basis of in situ geotechnical survey, the four-dimensional cross-correlation method was simplified to a two dimensional problem. This simple cross-correlation method was used to study the orientation of each downhole instrument by finding the maximum correlation coefficient from a different rotated angle in respect to the ground surface station. The results show the longitudinal directions of the downhole accelerometers at depths of 50 m, 100 m, and 200 m are N3°±7°E, N91°±10°E, and N75°±10°E, respectively.

Frequency dependent Q was calculated after the orientation correction, and the result of $Q(f)=9.55f^{1.06}$ was obtained from the smoothed power spectrum ratio. Shieh (1992) obtained $Q=55.11\pm15.10$ average from 1 to 22 Hz for Pleistocene sediment layer under the SMART1 array area. When frequency equal to 10 Hz, the Q value is 132.0 in SMART2 downhole array area. The Q value in Da-Han downhole array area is higher than that in Lotung area (SMART1 area). The geology and velocity logging data shows that the alluvium layer under the SMART1 array is softer than the gravel layer beneath the SMART2 downhole area, so, the higher Q value is reasonable.

The one-dimensional Haskell method was used to check the accuracy of the instrument orientations and Q value we obtained. The surface motions were simulated by using downhole records at depths of 50 m, 100 m, and 200 m as input motion. The results were good enough to prove the accuracy of instrument orientations and Q(f) value obtained in this study.

Acknowledgements We wish to thank Dr. H.-C. Chiu and the technical staff of the Institute of Earth Sciences who are responsible for the operation of the SMART2 array. The corrected accelerograms were prepared by Mr. W.-G. Huang and the data processing group. Comments by two anonymous reviewers are appreciated.

REFERENCES

Aki, K., 1980: Attenuation of shear-waves in the lithosphere for frequencies from 0.5 to 25 Hz. *Phys. Earth. Planet. Inter.*, **21**, 50-60.

Aki, K., and B. Chouet, 1975: Origin of coda waves: source, attenuation, and scattering effects. *J. Geophys. Res.*, **80**, 3322-3342.

Archuleta, B. J., S. H. Seale, P. V. Sangas, L. M. Baker, and S. T. Swain, 1992: Garner valley downhole array of accelerometers: instrumentation and preliminary data analysis. *Bull. Seis. Soc. Am.*, **82**, 1592-1621.

Bath, M., 1979: Spectral analysis in Geophysics. Elsevier Scientific Publishing Company, 463pp.

Carter, J. A., F. K. Duennebier, and D. M. Hussong, 1984: A comparison between a downhole seismometer and a seismometer on the ocean floor. *Bull. Seis. Soc. Am.*, **74**, 763-772.

Chang, L. S., and Y. T. Yeh, 1983: The Q value of strong ground motion in Taiwan. *Bull. Inst. Earth Sci., Academia Sinica*, **3**, 127-148.

Chiu, H. C., and Y. T. Yeh, 1992: A new strong-motion array in Taiwan-SMART2. General Assembly, IUGG, Book of IASPEI Abstracts, 132.

Chung-Chi Technical Consultant Co., 1991: Site soil boring and testing report of Jun-Kung Marble Plant and Da-Han Industrial School strong motion array. Chung-Chi Technical Consultant Co.,Taipei, Taiwan.

Console, R., and A. Rovelli, 1981: Attenuation parameters for Friuli region from strong-motion accelerogram spectra. *Bull. Seis. Soc. Am.*, **71**, 1981-1991.

Der, Z. A., and T. W. McElfresh, 1977: The relationship between anelastic attenuation and regional amplitude anomalies of short-period P waves in North America. *Bull. Seis. Soc. Am.*, **67**, 1303-1371.

Fletcher, J. B., T. Fumal, H-P. Liu, and L. C. Haar, 1990: Near surface velocity and attenuation at two boreholes near Anza, California, from logging data. *Bull. Seis. Soc. Am.*, **80**, 807-831.

Gibbs, J. F., and E. F. Roth, 1989: Seismic velocities and attenuation from borehole measurements near the Parkfield prediction zone central California. *Earthquake Spectra*, **5**, 513-537.

Hauksson, E., 1987: Seismotectonics of the Newport-Inglewood fault zone in the Los Angeles basin, southern California. *Bull. Seis. Soc. Am.*, **77**, 539-561.

Malin, P. E., J. A. Waller, R. D. Borcherdt, E. Granswick, E. G. Jensen, and J. Van Schaack, 1988: Vertical seismic profiling of Oroville microearthquakes: velocity spectra and particle motion as a function of depth. *Bull. Seis. Soc. Am.*, **78**, 401-420.

Rautian, T. G., and V. I. Khalturin, 1978: The use of the coda for determination of the earthquake source spectrum. *Bull. Seis. Soc. Am.*, **68**, 923-948.

Rodriguez, M., J. Havskov, and S. K. Singh, 1983: Q from coda waves near Petatlan, Guerrero, Mexico. *Bull. Seis. Soc. Am.*, **73**, 321-326.

Seale, S. H., and R. J. Archuleta, 1989: Site amplification and attenuation of strong ground motion. *Bull. Seis. Soc. Am.*, **79**, 1673-1696.

Shieh, C. F., 1992: Estimation of Q value by SP/S spectral ratio. *TAO*, **3**, 469-482.

Tsujiura, M., 1978: Spectral analysis of the coda waves from local earthquakes. *Bull. Earthq. Res. Inst., Univ. Tokyo*, **53**, 1-48.

Vidale, J. E., 1986: Complex polarization analysis of particle motion. *Bull. Seis. Soc. Am.*, **76**, 1393-1405.

Wang, J. H., 1993: Q value of Taiwan: a review. *J. Geolog. Soc. China*, **36**, 15-24.

Yamazaki, F., L. Lu, and T. Katayama, 1992: Orientation error estimation of buried seismographs in array observation. *Earthq. Eng. Struct. Dyn.*, **21**, 679-694.